Available online at www.eccomasproceedia.org
Eccomas Proceedia COMPDYN (2023) 4683-4692

ECCOMAS Proceedia

COMPDYN 2023
9th ECCOMAS Thematic Conference on
Computational Methods in Structural Dynamics and Earthquake Engineering
M. Papadrakakis, M. Fragiadakis (eds.)
Athens, Greece, 12-14 June 2023

NUMERICAL SEISMIC PERFORMANCE INVESTIGATION OF AAC INFILL WALLS WITH FLAT-TRUSS BED-JOINT REINFORCEMENT

Omer Faruk Halici[1,2] **and Alper Ilki**[2]

[1] MEF University, Department of Civil Engineering
e-mail: halicio@mef.edu.tr

[2] Istanbul Technical University, Faculty of Civil Engineering
e-mail: halici@itu.edu.tr
e-mail: ailki@itu.edu.tr

Abstract

Autoclaved Aerated Concrete (AAC) is a lightweight, energy-efficient and easy-to-transport material. As a result, AAC walls are becoming increasingly common as an infill solution in earthquake-prone areas such as Turkey, Italy, and Greece. Although infills are considered as secondary components in seismic design, they are extremely vulnerable to damage during earthquakes along both in-plane (IP) and out-of-plane (OOP) directions. Previous post-earthquake site examinations revealed that the failure of infill walls can result in serious injuries and casualties. Furthermore, huge economic losses as well as disruption in the functionality of essential buildings that are supposed to be operational after earthquakes may adversely affect the daily life in the earthquake-affected regions. One of the potential methods for increasing the seismic resilience of infill walls is use of bed-joint reinforcement between infill courses. In this paper, the general approaches in the establishment of the numerical finite element model for infill walls with and without bed-joint reinforcement are presented. The developed model was evaluated according to the previous full-scale experimental test results from strength and damage propagation point of view. The model will be used to investigate the response of infills with various bed-joint reinforcement amounts and height-to-length ratios to generalize the seismic performance improvements obtained by the use of flat-truss reinforcement both in the IP and OOP directions.

Keywords: Infill wall, Autoclaved Aerated Concrete (AAC), bed-joint reinforcement, seismic response

---

ISSN:2623-3347
Peer-review under responsibility of the organizing committee of COMPDYN 2023.
doi: 10.7712/120123.10750.20826

1 INTRODUCTION

In typical structural systems like reinforced concrete (RC), steel, masonry, etc., infill walls are generally benefitted as separators and thermal insulators. However, these components are typically made of brittle materials and are not given enough attention in structural design procedures, without adequate safety assessments. Recent earthquakes, such as the 2009 L'Aquila, 2011 Van, and 2020 Izmir earthquakes, have highlighted the potential for infill walls to be subjected to severe damages, resulting in significant injuries and loss of life [1-10]. Additionally, the failure of an infill wall can cause significant damage to non-structural elements and expensive equipment in critical facilities such as hospitals, laboratories, and offices, which can disrupt their functionality in the aftermath of earthquakes.

Autoclaved aerated concrete (AAC) is a construction material that is gaining popularity in seismic regions due to its attractive properties such as being precast, lightweight, fire-resistant and energy-efficient, and is one of the widely used materials in infill walls. AAC is a cementitious material that has visible closed air voids providing its low density, which is an advantageous feature to reduce seismic inertia forces. Material properties of AAC are presented in Table 1.

Table 1: Mechanical properties of AAC

Characteristic		AAC
Unit weight	(kg/m^3)	400 to 800
Compressive strength	(MPa)	2.0 to 7.6
Moisture content after autoclaving	(%)	30
Moisture content in use	(%)	5 to 15
Coefficient of thermal expansion	(/°C)	8.1 x 10^{-6}
Coefficient of creep	(/ MPa)	0.72 x 10^{-4}

The use of bed-joint reinforcement is one of the most promising solutions to enhance the seismic performance of infill walls. Experimental studies have been conducted to investigate the benefits of using bed-joint reinforcements in infill walls made of clay brick and AAC blocks. Calvi and Bolognini [11] evaluated the in-plane (IP) and out-of-plane (OOP) seismic performance of enhancement of infills made of hollow clay bricks. Penna et.al. [12-13] and Penna and Calvi [14] studies investigated and revealed the benefits of using bed-joint reinforcements to enhance the IP and OOP seismic performance of AAC walls.

This paper presents the numerical study performed to investigate the seismic response of AAC infill walls with and without bed-joint reinforcement that are constructed in RC frames. Previous experimental tests investigating the IP and OOP response of unreinforced and bed-joint reinforced AAC infill walls [15] are benefitted to critically evaluate the model performance from strength and damage propagation point of view. The model adequateness and deficiencies are presented.

2 TEST PARAMETERS AND EXPERIMENTAL RESULTS

Full-scale experimental tests were performed at Istanbul Technical University Structural and Earthquake Engineering Laboratory. AAC infill walls in RC frames with and without steel flat-truss reinforcements were tested in IP and OOP directions. The matrix of numerically evaluated specimens is presented in Table 2. All specimens were tested in the OOP direction. One specimen of the unreinforced-type specimen and truss-type reinforced specimens were imposed to an IP drift of 0.005 before tested in the OOP direction. The plan view of truss-type reinforced infill courses is presented in Figure 1. The specimen geometry, RC reinforcement details and the location of the bed-joint reinforced courses in truss-type reinforced specimens are presented in Figure 2.

Table 2: Specimen properties

Specimen Name	Infill Material	Prior In-plane Drift Ratio	Bed-Joint Reinforcement
W_Ref	AAC	-	Unreinforced
W_Ref_PIP_0.005	AAC	0.005	Unreinforced
W_ Truss _PIP_0.005	AAC	0.005	Flat-truss

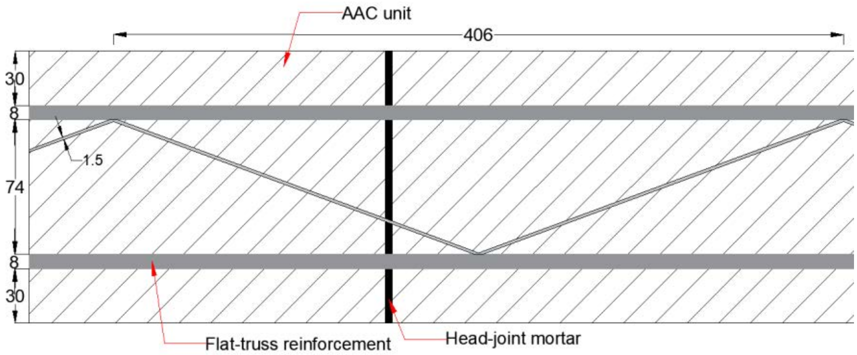

Figure 1: Plan view of truss-type reinforced infill course

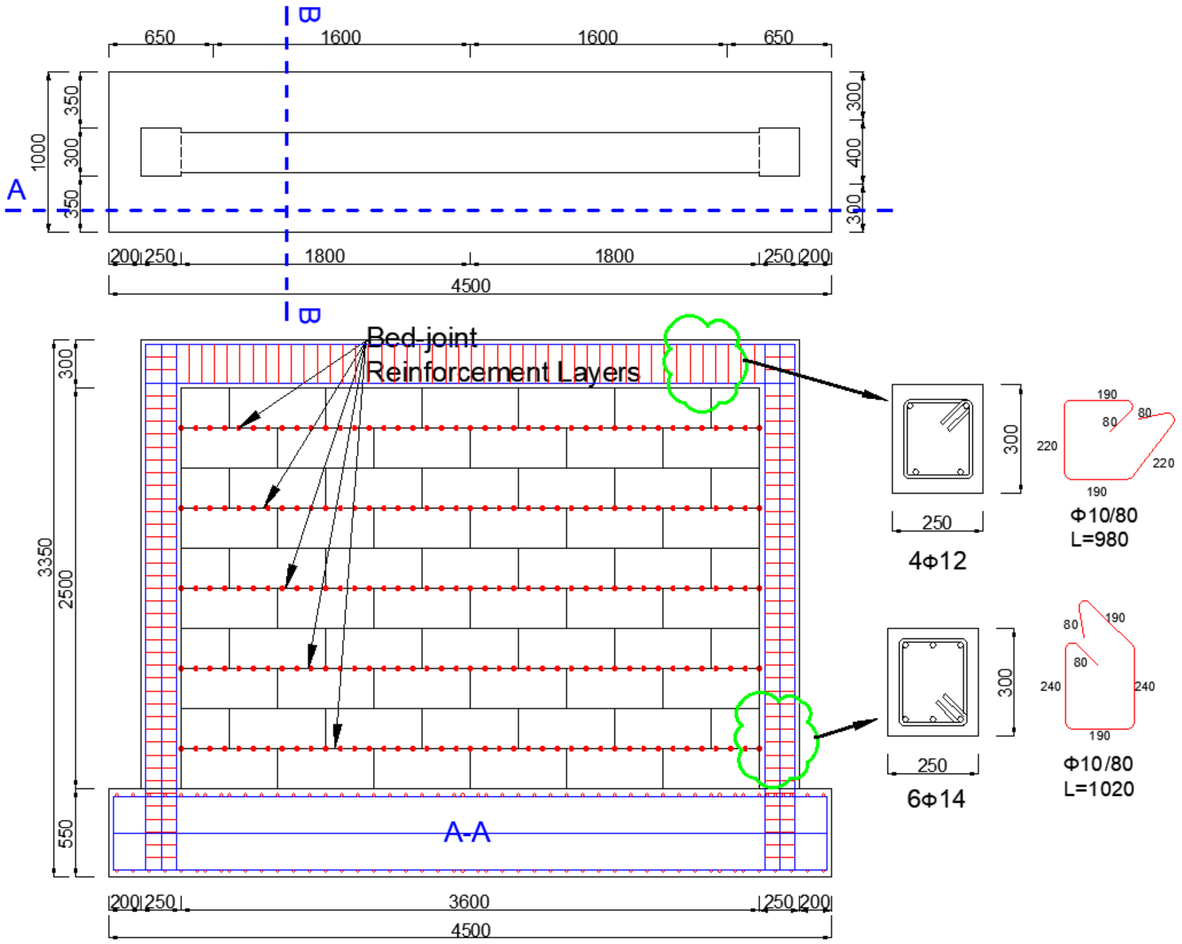

Figure 2: Specimen geometry [mm]

All infill walls were constructed with AAC 2.50 strength-class blocks having dimensions of 600×250×150 mm and 300x250x150 mm (length×height×thickness). M10 strength-class thin layer mortar with a thickness of 2 mm was used in the head and bed joints of adjacent AAC blocks in unreinforced specimens. In the reinforced courses of truss-type reinforced specimen, the mortar thickness was 4 mm. In all specimens, there was a 15 mm gap between the top of the AAC infills and the bottom of the RC beams, which was filled with polyurethane spray foam. The loading protocols followed in the IP and OOP tests are presented in Figure 3. The IP tested specimens were imposed to cyclic reversal displacements up to 0.005 drift ratio corresponding to 13.25 mm displacement. The OOP displacements up to 160 mm were applied to the specimens via a 4-point loading apparatus. The OOP displacements were applied at one-third of the length and height of the specimens. The IP and OOP backbone curves of the specimens are presented in Figure 4.

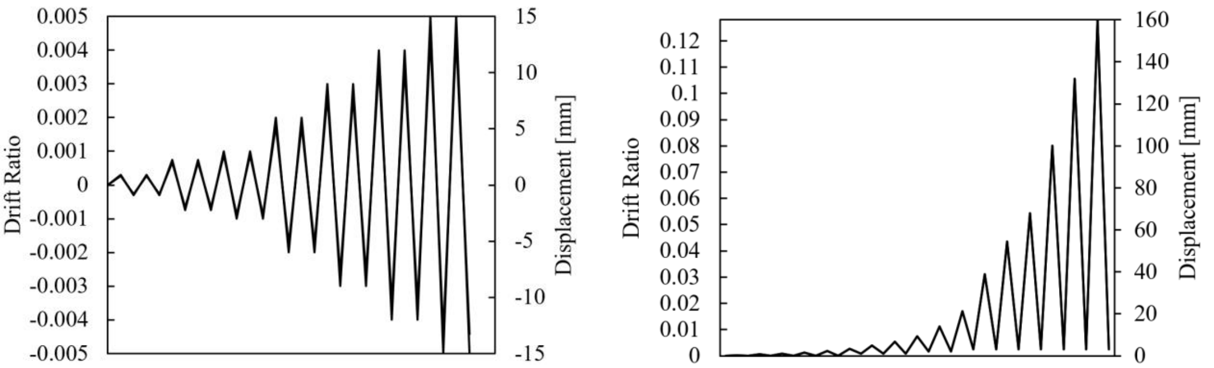

(a) (b)

Figure 3: Loading protocols: (a) IP cyclic loading protocol; (b) OOP loading protocol

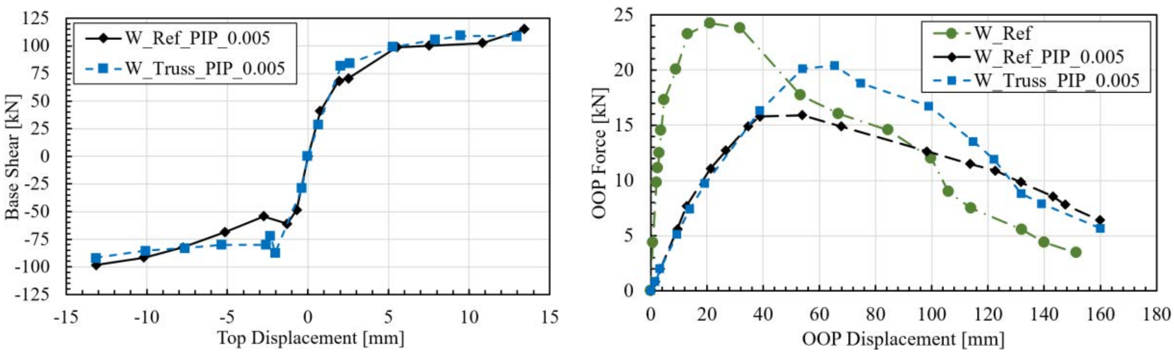

(a) (b)

Figure 4: Backbone curves: (a) Response in IP direction; (b) Response in OOP direction

3 MODELING METHODOLOGY

A numerical 3D Finite Element Model (FEM) was developed in Abaqus 2020 software [16]. Explicit solver was used, and quasi-static dynamic analyses were performed. Simplified micro modeling method was adopted since the mortar thicknesses at the AAC-AAC and AAC-RC Frame interfaces were very thin (1-3 mm) to be modeled as separate elements as in micro modeling approach. Instead, the behavior of joints between the infill units were represented by contact elements. Three-dimensional 8-node hexahedral continuum finite elements with reduced integration (C3D8R) were used in the modeling of RC frame, AAC blocks and the top foam. 2-node linear truss elements (T3D2) were used to model the reinforcements. Elastic-perfectly plastic material models were used for the RC rebars and the bed-joint reinforcements. The reinforcements were embedded to the concrete and AAC elements and bond slip response was not taken into account. The cyclic IP displacement reversal protocol presented in Figure 3a was defined in the model accordingly. However, the OOP displacements were imposed monotonically.

3.1 Material Properties

Concrete Damaged Plasticity (CDP) model was adopted to represent the compressive and tensile response of concrete material. The mean concrete compressive strength used in the RC frame was experimentally determined as 29.4 MPa. The material model is defined accordingly. The typical uniaxial response of concrete under compressive and tensile stresses modeled with CDP are presented in Figure 5 [16]. E_0 is the undamaged stiffness of the material and $\varepsilon_c^{\sim pl}$, $\varepsilon_t^{\sim pl}$, $\varepsilon_c^{\sim in}$, $\varepsilon_t^{\sim in}$ are compressive plastic strain, tensile plastic strain, compressive inelastic strain and tensile inelastic strain, respectively. CDP model weakens the unloading stiffness of the material as the material takes inelastic strain. Two damage parameters are used to define the unloading stiffness values: d_c and d_t which are valued between zero and one. Zero represents the undamaged condition of the material, while one represents the total failure. The damage parameters are determined according to the methodology proposed by Alfarah et al. [17] which takes into account the characteristic length (l_{eq}) of the mesh elements. The characteristic length is obtained by dividing the element volume by the largest area of mesh faces. Since the RC frame is made of cubic mesh elements with a size of 50 mm, l_{eq} is 50 mm. The compressive and tensile stress-plastic strain relationships are presented in Figure 6. Other CDP parameters are presented in Table 3. E_0, ν, K_c, f_{b0}/f_{c0} and ε stand for the undamaged modulus of elasticity, Poisson's ratio, the ratio of second stress invariants on tensile and compressive meridians, the ratio of biaxial compressive strength to uniaxial compressive strength and eccentricity of the plastic potential curve, respectively. The RC frame is modeled as one unified part. The mean tensile strengths of the reinforcement used in the RC frame were experimentally obtained as 476.4 MPa and 523.3 MPa for longitudinal and transversal reinforcements, respectively.

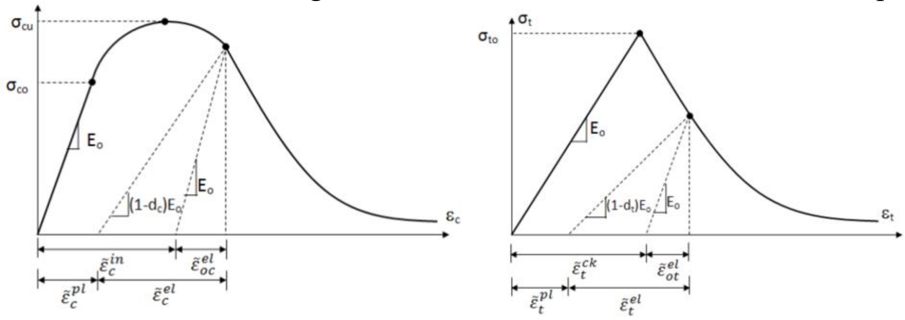

(a) (b)

Figure 5: Stress-strain response of concrete under: (a) compression; (b) tension

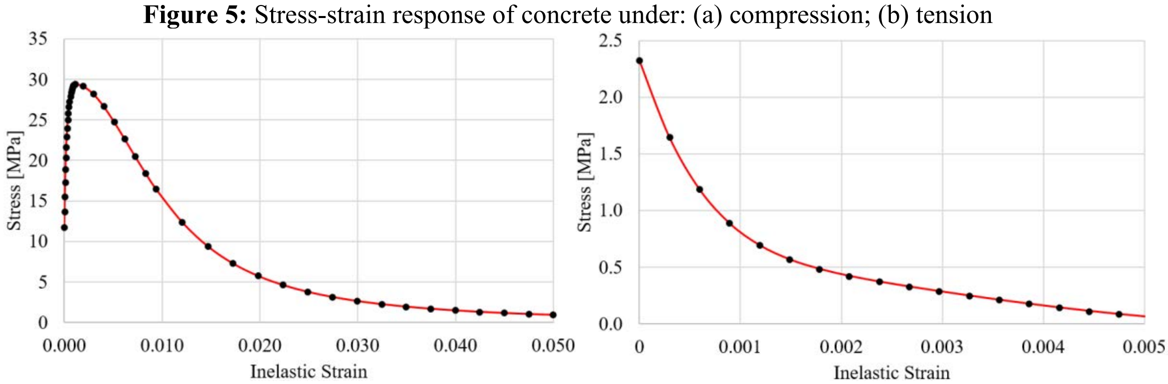

(a) (b)

Figure 6: Stress-strain relationships for concrete, l_{eq}=50 mm: (a) Compression; (b) Tension

Table 3: CDP parameters for concrete

E_0 [MPa]	*ν*	*K_c*	*Dilatancy Angle Ψ [°]*	*f_{b0}/f_{c0}*	*ε*
30863	0.2	0.667	13	1.16	0.1

The mean compressive strength of AAC infill units was experimentally obtained as 2.54 MPa. Past experimental tests performed by Turkish Autoclaved Aerated Concrete Association (TAACA) indicated that the tensile strength, mean modulus of elasticity and the strain at the peak compression stress for AAC 2.50 were obtained as 0.135 MPa, 990 MPa and 0.0035, respectively. Based on this data and the model developed by Thorenfeldt et.al. [18] the compression and tensile stress-strain relationships for AAC were determined (Figure 7). The damage parameters for AAC were determined according to the methodology suggested by Birtel and Mark [19].

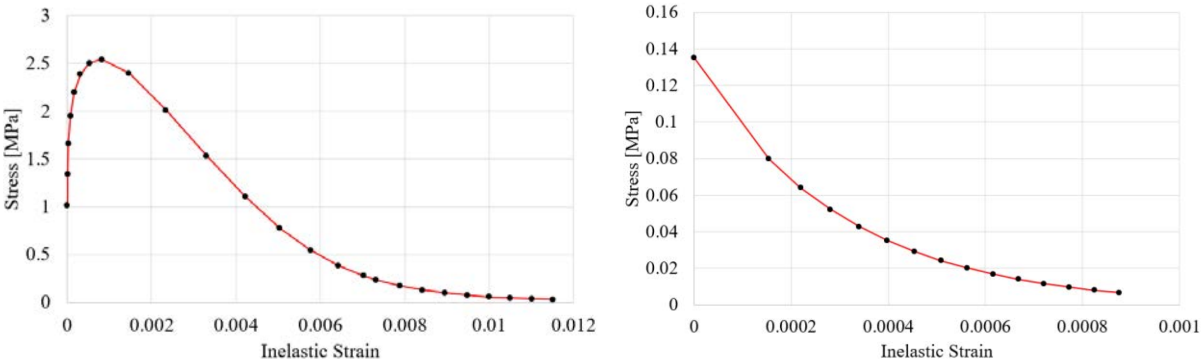

(a) (b)

Figure 7: Stress-strain relationships for AAC: (a) Compression; (b) Tension

In order to represent the contact conditions between the infill and the RC frame, the polyurethane foam at the uppermost bed-joint of the infill specimens was included in the model. The foam fills the gap between the top of the wall and the RC beam. The density of the foam was 40 kg/m^3. During the specimen production, the thickness of the foam was measured as 15 mm. Ogden's model [20] was benefitted to represent the polyurethane foam in the FEM model.

3.2 Interaction Properties

A cohesive traction-separation relationship was defined to represent the behavior of bed-joint mortar between AAC infill units and AAC-RC frame interfaces where M10 mortar with an average thickness of 2 mm was used in the construction of the specimens. From the triplet tests performed by TAACA, the average shear stress where slip starts between AAC 2.50 units with M10 mortar was recorded as 0.18 MPa. Also, the friction coefficient measured in these tests was calculated as 0.62. The interface properties used in the model are presented Table 4. The interface between AAC and polyurethane foam, together with RC frame and polyurethane foam was assumed to be perfectly bonded. A tie constraint was assigned to those surfaces. The model assembly and the interactions between the model components were presented in Figure 8.

Table 4: Mechanical properties of joint interfaces

Tensile Strength f_t [MPa]	*Shear Strength f_s [MPa]*	*μ*	*K_{nn} [N/mm^2/mm]*	*K_{ss} [N/mm^2/mm]*	*G_F [N/mm]*
0.30	0.18	0.62	100	40	0.02

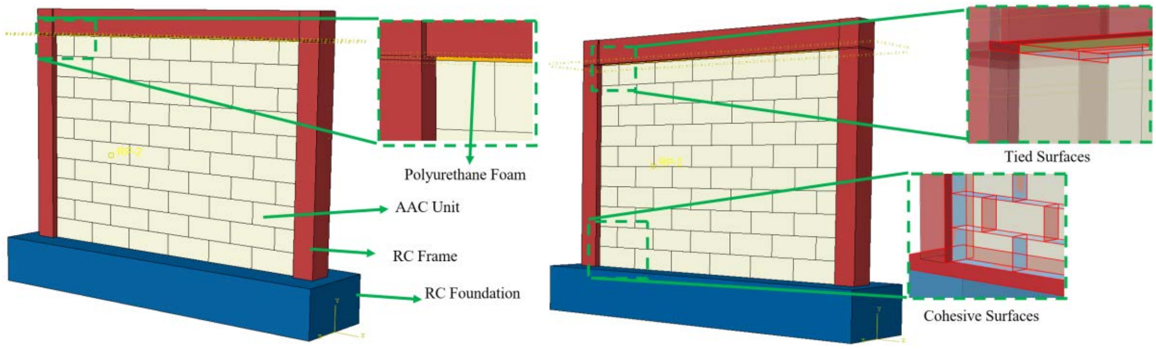

Figure 8: (a) model assembly; (b) contact properties in different parts

4 MODEL EVALUATION

Numerical analyses were carried out according to the IP and OOP loading protocols applied to the specimens during the experimental tests. The comparison of experimental and numerical damage propagation of W_Ref_PIP_0.005 during the IP loadings is presented for two IP drift levels (i.e., 0.001 and 0.002) in Figure 9. The damage states obtained from the numerical analyses at these imposed drift levels are coherent with the damages observed during the experimental tests.

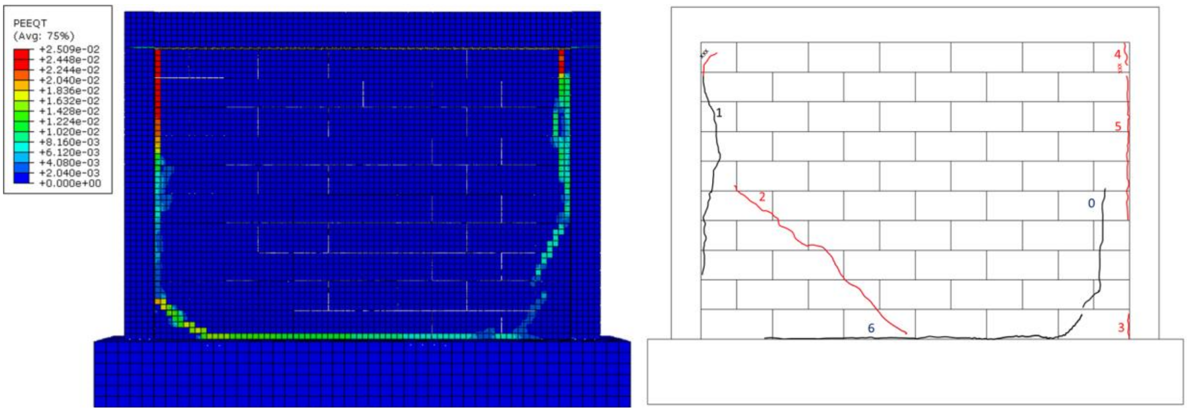

(a)

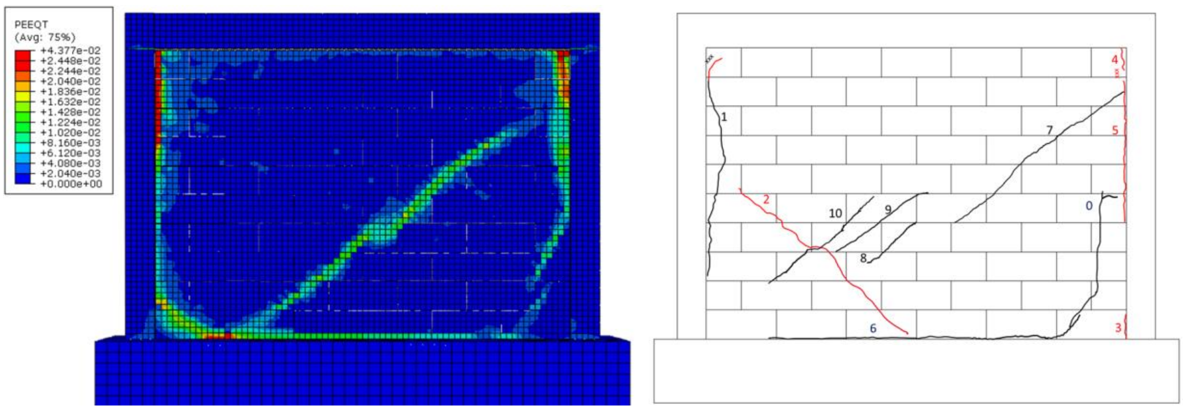

(b)

Figure 9: Numerically calculated plastic strains (PEEQT) versus experimentally observed cracks on W_Ref_PIP_0.005: (a) at 0.001 IP drift ratio; (b) at 0.002 IP drift ratio

The obtained OOP force-displacement relationships are presented in Figure 10. The adopted numerical modeling approach reveals the potential to represent the approximate OOP capacity of the infills with a variation of 10%. Yet, the initial stiffness responses obtained from the numerical analyses for the prior IP damages specimens (i.e., W_Ref_PIP_0.005 and W_Truss_PIP_0.005, shown in Figure 10a,b, respectively) do not seem to be coherent with the experimental response. Further optimization of the numerical modeling approach is needed.

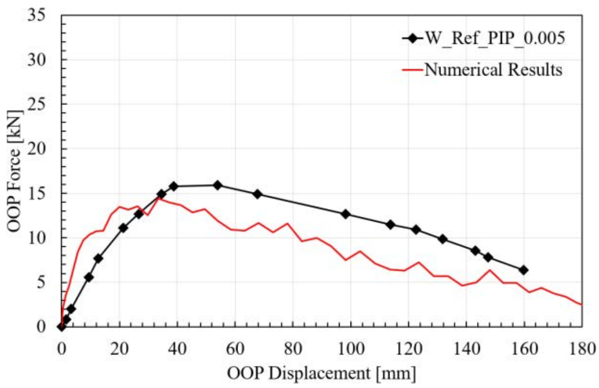

(a)

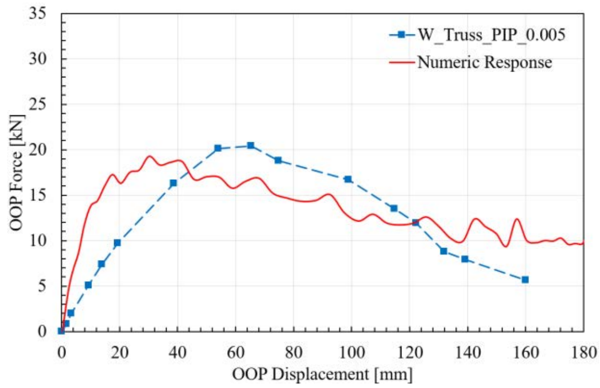

(b)

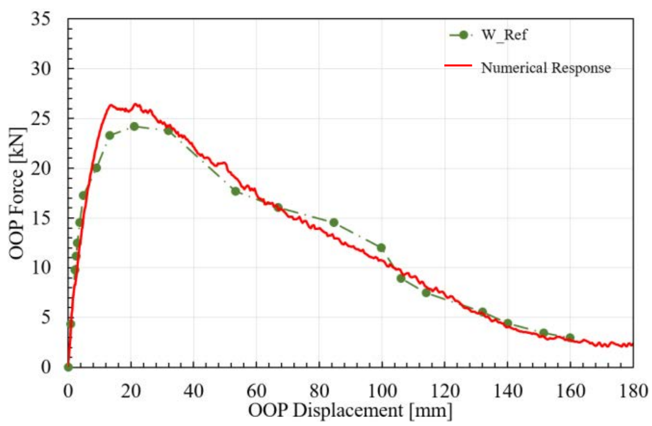

(c)

Figure 10: Experimental vs numerically obtained OOP force-displacement relationships: (a) W_Ref_PIP_0.005; (b) W_Truss_PIP_0.005; (c) W_Ref

5 CONCLUSION

In this paper, the numerical modeling approach with a potential of successfully representing the IP and OOP response of AAC infills is presented. Simplified micro modelling approach was utilized since the mortar layers between AAC units are considerably thin to be modeled as separate elements. The mortar response was represented by a cohesive traction and separation law defined at the AAC interfaces. Concrete damaged plasticity model was used to model the non-linear response of AAC units and RC members, which were modeled with 3D finite elements. The response obtained from this modeling approach indicates a great potential to represent the IP and OOP response of AAC infills together with the OOP response of prior IP damaged infills. Yet, further developments are needed to successfully represent the OOP stiffness of the IP damaged infill walls. Once it is established and validated, the modeling approach will be used to generalize the experimental findings and to investigate the response of various infill configurations including height/length ratio, height/thickness ratio, reinforcement amount and prior IP drift level etc.

6 REFERENCES

[1] A. Ceci, A. Contento, L. Fanale, D. Galeota, V. Gattulli, M. Lepidi et al., Structural performance of the historic and modern buildings of the University of L'Aquila during the seismic events of April 2009. *Engineering Structures*. **32**, 1899-924, 2010.

[2] P. Ricci, F. De Luca, G.M. Verderame, 6th April 2009 L'Aquila earthquake, Italy: reinforced concrete building performance. *Bulletin of Earthquake Engineering*. **9**, 285-305, 2011

[3] F. Braga, V. Manfredi, A. Masi, A. Salvatori, M. Vona, Performance of non-structural elements in RC buildings during the L'Aquila, 2009 earthquake. *Bulletin of Earthquake Engineering*. **9**, 307-24, 2011

[4] M. Tapan, M. Comert, C. Demir, Y. Sayan, K. Orakcal, A. Ilki. Failures of structures during the October 23, 2011 Tabanlı (Van) and November 9, 2011 Edremit (Van) earthquakes in Turkey. *Engineering Failure Analysis*. **34**, 606-28, 2013.

[5] M. Di Ludovico, A. Prota, C. Moroni, G. Manfredi, M. Dolce. Reconstruction process of damaged residential buildings outside historical centres after the L'Aquila earthquake: part I—" light damage" reconstruction. *Bulletin of Earthquake Engineering*. **15**, 667-92, 2017.

[6] M. Di Ludovico, A. Prota, C. Moroni, G. Manfredi, M. Dolce. Reconstruction process of damaged residential buildings outside historical centres after the L'Aquila earthquake: part II—"heavy damage" reconstruction. *Bulletin of Earthquake Engineering*. **15**, 693-729, 2017.

[7] B. Yön, O. Onat, M.E. Öncü. Earthquake damage to nonstructural elements of reinforced concrete buildings during 2011 Van seismic sequence. *Journal of Performance of Constructed Facilities*. **33**, 04019075, 2019.

[8] A. Yakut, H. Sucuoğlu, B. Binici, E. Canbay, C. Donmez, A. İlki et al. Performance of structures in İzmir after the Samos island earthquake. *Bulletin of Earthquake Engineering*. 1-26, 2021.

[9] T. Gurbuz, A. Cengiz, S. Kolemenoglu, C. Demir, A. Ilki. Damages and Failures of Structures in İzmir (Turkey) during the October 30, 2020 Aegean Sea Earthquake. Journal of Earthquake Engineering. 1-42, 2022.

[10] H. Varum, A. Furtado, J. Melo. Insights on the Seismic Design of Current RC Buildings: Field Lessons, Codes and Research Needs. *European Conference on Earthquake Engineering and Seismology,* Springer, 2022. p. 311-22.

[11] G. M. Calvi, and D. Bolognini. Seismic response of reinforced concrete frames infilled with weakly reinforced masonry panels. *Journal of Earthquake Engineering,* **5**,153-185, 2001.

[12] A. Penna, G. Magenes, G.M. Calvi, A.A. Costa. Seismic performance of AAC infill and bearing walls with different reinforcement solutions. Proceedings of the 14th International Brick and Block Masonry Conference, 2008. p. 13-20.

[13] A. Penna, M. Mandirola, M. Rota, G. Magenes. Experimental assessment of the in-plane lateral capacity of autoclaved aerated concrete (AAC) masonry walls with flat-truss bed-joint reinforcement. *Construction and Building Materials*. **82**,155-66, 2015.

[14] A. Penna, G. Calvi. Campagna sperimentale su telai in ca con tamponamenti in Gasbeton (AAC) con diverse soluzioni di rinforzo. Experimental report, University of Pavia, Italy (in Italian). 2006.

[15] O.F. Halici, U. Demir, Y. Zabbar, A. Ilki. Out-of-Plane Seismic Performance of Bed-Joint Reinforced Autoclaved Aerated Concrete (AAC) Infill Walls Damaged under Cyclic In-Plane Displacement Reversals. *Engineering Structures,* **286**,116077, 2023.

[16] Simulia. Abaqus FEA. Dassault Systemes Simulia Corporation. 2020.

[17] B. Alfarah, F. López-Almansa, S. Oller. New methodology for calculating damage variables evolution in Plastic Damage Model for RC structures. *Engineering Structures*. **132**, 70-86, 2017.

[18] E. Thorenfeldt, A. Tomaszewicz, J. J. Jensen. Mechanical properties of high-strength concrete and application in design. *Symposium on Utilization of High-Strength Concrete*. Trondheim, Norway. 1987. p. 149-159.

[19] V.A. Birtel, P. Mark. Parameterised finite element modelling of RC beam shear failure. *ABAQUS users' conference.* 2006.

[20] R.W. Ogden. Large deformation isotropic elasticity–on the correlation of theory and experiment for incompressible rubberlike solids. *Proceedings of the Royal Society of London. A. Mathematical and Physical Sciences*, **326(1567)**, 565-584, 1972.